

# MEASUREMENTS OF THE LOCALIZED STATE ELECTRONIC STRUCTURE OF ORGANIC SOLAR CELLS

R. A. Street and K. W. Song  
Palo Alto Research Center, Palo Alto, CA 94304

## ABSTRACT

Experimental measurements of the band tail density of states distribution in bulk heterojunction solar cells, are described, with measurements made on P3HT:PCBM and PCDTBT:PCBM. The transient photoconductivity experiment measures the electron and hole drift mobility in the solar cells. The dispersive nature of the electronic transport is directly related to the band tail density of states distribution. The technique is extended to measure the band tail DOS over a range of energies. In each type of cell we observe an approximately exponential band tail, but also find an additional broad distribution of deep states. Measurements of the photocurrent spectral response to low energy provide an alternative measure of the optical absorption spectrum for excitations from the polymer HOMO to the PCBM LUMO. These data also reveal an exponential distribution of band tail states with a slope that is the same as the electron transport measurements.

## INTRODUCTION

Organic bulk heterojunction solar cells are a phase separated blend of an electron donor and acceptor [1]. Understanding the transport and recombination mechanisms that determine the cell efficiency is important to be able to model the cell, find materials and structures to improve the efficiency and to understand the effects of annealing and environmental exposure. Since the cells are fabricated with disordered materials, the role of localized states is particularly important. Disordered semiconductors are well known to have a band tail of localized states and often also deeper trap states.

Annealing usually improves the cell performance by increasing the structural order of the organic materials, and adsorption of water, ozone and other gas impurities often introduces trap states that degrade performance. Both effects change the electronic transport and recombination processes and hence the cell efficiency. However, the direct link between the cell processing history and cell performance has not been demonstrated because experimental techniques have not previously been available to measure the details of the electronic structure. Of particular interest is the distribution of localized trapping states because of their important role in electronic transport and recombination. This paper describes techniques that allow measurement of the density of states distribution which is essential information to be able to model cell performance. Furthermore, the techniques provide a tool to measure and quantify the

changes that occur after cell processing and environmental exposure.

## EXPERIMENTAL METHODS

The photoconductivity spectral response experiment uses a 0.25 m grating spectrometer with a halogen light source. The cell circuit has a 9 kohm load resistor so that the measurement is of photocurrent rather than photovoltage. The voltage across the load is measured with a lock-in amplifier with illumination chopped at 230 Hz. Filtering out stray light from the monochromator is essential to obtain a high dynamic range measurement.

The transient photoconductivity measurement uses a nitrogen pumped pulsed dye laser emitting a short light pulse at a wavelength of  $\sim 520\text{nm}$ . The current is measured from the voltage drop across a load resistor, which varied from 4 to 9000 ohm depending on the time scale of interest, and is recorded on a digital oscilloscope. The measurements were made with a  $\sim 1\text{ Hz}$  repetition rate to allow any trapped charge to disperse, and the current transient is an average of up to 64 measurements.

## TRANSIENT PHOTOCONDUCTIVITY

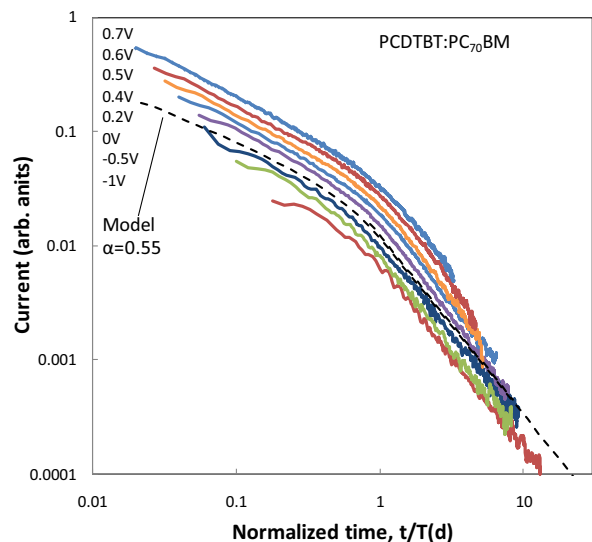


Figure 1. The transient photoconductivity data of PCDTBT:PCBM, with the time scaled to correspond to the normalized transit time  $T(d)$ . The dashed line is a fit to the dispersion model with parameter  $\alpha=0.55$ .

Figure 1 shows transient photoconductivity data for a PCDTBT:PCBM solar cell [2]. Since the solar cell is only about 100 nm thick and the optical absorption depth is about the same, the measured current is the sum of contributions from electrons and holes. As described elsewhere the two components can be separated by their different time response [2]. The data in Figure 1 is for the slower of the two carriers, and is experimentally identified to be holes in the polymer [3, 4]. The current transient is dispersive, as shown by the power law time dependence with a change of slope at the transit time.

The data are measured at different applied bias as shown and are scaled in time to a fixed transit time. This procedure more clearly identifies the power law time dependence and the change of slope at the transit time. The scaling factor provides the voltage dependence of the transit time from which the mobility is obtained. An analysis that includes the carrier profile allows us to measure the mobility and also obtain the dispersion in the transport, based on a model described elsewhere [1].

A common mechanism for carrier dispersion is multiple trapping in an exponential distribution of band tail states proportional to  $\exp(-(E-E_M)/E_T)$ , where  $E_M$  is the transport energy and  $E_T$  is the band tail slope. The model assumes a discrete transport energy separating mobile and trapping states and also that carriers are thermally excited from the traps to the mobile states. When  $E_T > kT$  this model predicts dispersive transport with dispersion parameter [5],

$$\alpha = kT/E_T. \quad (1)$$

Figure 2 shows the temperature dependence of the dispersion parameter for P3HT:PCBM cells which confirm this relation. The transient photocurrent measurements give values for the band tail slope of  $E_T$  of  $\sim 0.045 \pm 0.005$  eV and  $\sim 0.033 \pm 0.007$  eV for the PCDTBT:PCBM and P3HT:PCBM solar cells respectively, based on the measurements of the dispersion parameter.

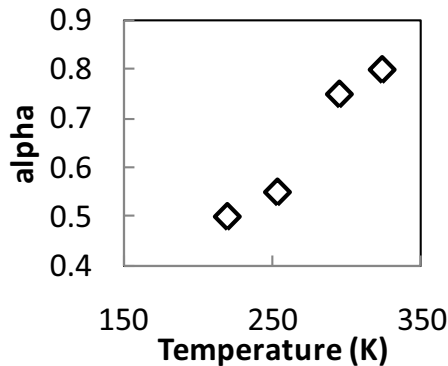


**Figure 2. Temperature dependence of the dispersion parameter  $\alpha$ , showing that it conforms to Eq. 1.**

## Extended time transient photoconductivity

More detailed information about the localized state distribution is obtained by observing the long time response of the transient photoconductivity,  $I_{PC}(t)$ . We show elsewhere [3] that provided the density of states  $N(E)$  is reasonably broad compared to  $kT$ , the time dependence of the photocurrent is related to the density of states by the expressions,

$$N(E) \sim t \cdot I_{PC}(t), \text{ with } E = kT \ln(\omega t) \quad (2)$$

where  $\omega$  is an attempt-to-escape prefactor and provided that all the traps are filled by the excitation illumination. These relations arise since the excitation rate out of the deep traps is much slower than the carrier transit time. Hence the current at a specific time maps onto the density of states at a specific trap energy.

Figure 3 shows the transient photocurrent response for a PCDTBT:PCBM cell, extending nearly six orders of magnitude in time to 30 ms. The data comprises several separate measurements using progressively increasing load resistance. After the transit time at about  $1 \mu\text{s}$ , the current decreases with the same power law slope as in Fig. 1. However at about  $100 \mu\text{s}$ , there is a decrease in the slope, indicating a change in the shape of the density of states distribution. The inset to Fig. 3 shows that the photocurrent saturates at high excitation levels, indicating that there is complete trap filling. The measurement at a low illumination level shown in Figure 3 removes the small space charge effect at short times.

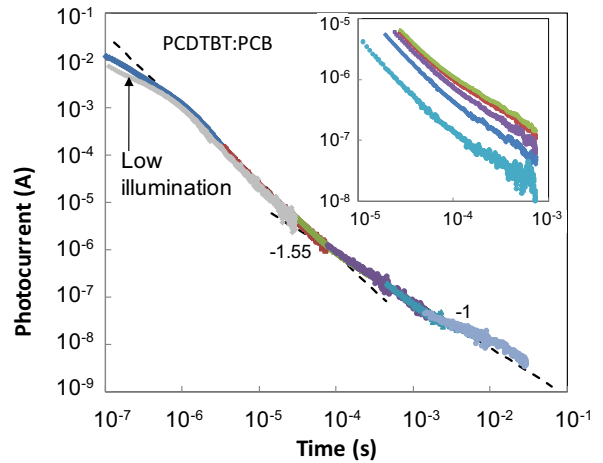


**Figure 3. Measurement of the transient photocurrent at extended times well beyond the transit time. Dashed lines are the power law slopes for the different regions. The inset shows the data near the change of slope as a function of light intensity, showing saturation.**

Figure 4 shows the density of states (DOS) distribution obtained from the data of Fig. 3 and from equivalent data for P3HT:PCBM, applying the model of eq. 2 and assuming that  $\omega$  is  $10^{11} \text{ s}^{-1}$ . Up to a trap energy of 0.4 eV,

the same band tail slope is obtained as from the dispersive mobility analysis, as expected. The distinct change of slope at longer times corresponds to a change in the DOS at trap energy above 0.4 eV. In the case of PCDTBT:PCBM, the deep DOS is relatively flat as a function of energy, while in P3HT:PCBM we observe a transition to a broader exponential tail, with a slope of about 65 meV. The DOS at a trap depth of 0.5 eV is  $10^{16}$ - $10^{17}$  cm<sup>-3</sup>eV<sup>-1</sup> for the two types of cell.

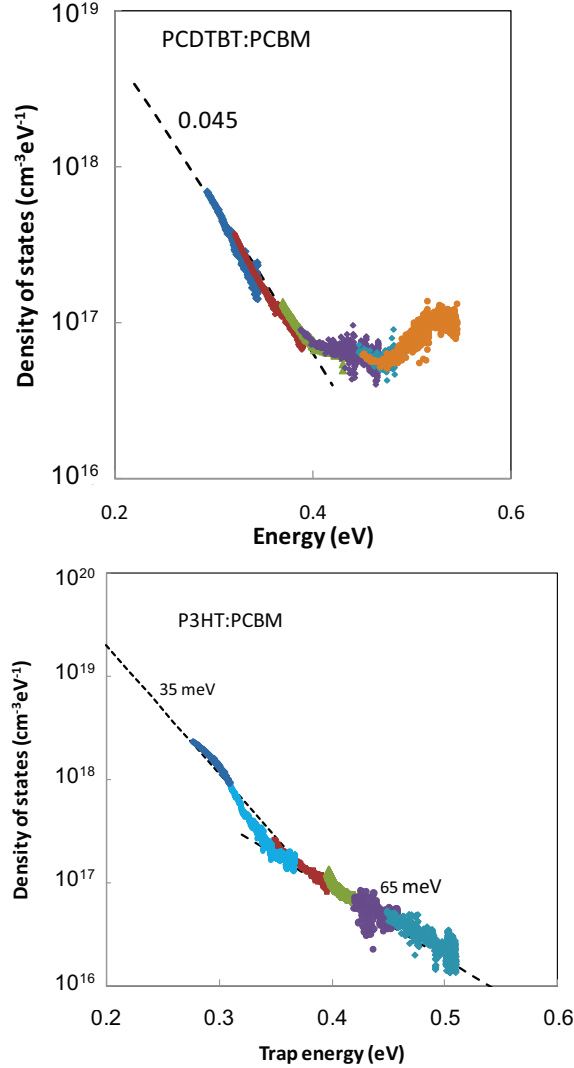


Figure 4. Density of states distribution for (upper) PCDTBT:PCBM and (lower) P3HT:PCBM, obtained from the transient photocurrent data as in Fig 3.

## PHOTOCURRENT SPECTRAL RESPONSE

The spectral response of the solar cells corresponds to optical excitations that create mobile carriers. At low photon energy, transitions from deep localized states to higher energy mobile states create a photocurrent. Hence

the low energy spectral response also gives information about the DOS of localized states.

Fig. 5 shows the photoconductivity spectral response of both types of cell measured down to 0.8 eV [3]. The photocurrent is the product of the optical absorption and the cell quantum efficiency. Independent measurements show that the quantum efficiency does not change significantly at low energy [5], so the measurement is primarily of the absorption coefficient, as shown in the vertical axis scale. The optical absorption coefficient,  $\alpha_T(\hbar\omega)$ , evaluated assuming an effective bulk absorption, is obtained from the photocurrent,  $I_{PC}(\hbar\omega)$  by,

$$I_{PC}(\hbar\omega) = I_0 (1 - \exp(-\alpha_T(\hbar\omega)d)) \quad (3)$$

where  $I_0$  is the photoconductivity at full absorption, and  $d$  is the effective cell thickness. For small values of  $\alpha_T d$ ,  $\alpha_T(\hbar\omega)d = I_{PC} / I_0$ . Our analysis uses an experimentally determined value of  $I_0$ . Although the absorption occurs at or near the domain interface, it is convenient to express it as an effective bulk absorption coefficient, since the exact internal interface area is not known.

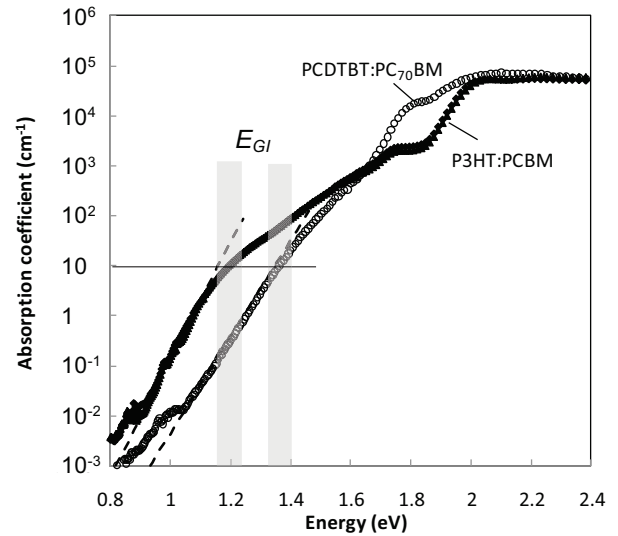


Figure 5. Optical absorption coefficient for the two types of cell, obtained from spectral response data [3]. The vertical shaded bands indicate the estimated interface optical band gaps  $E_{GI}$  for the two types of cell.

The optical absorption coefficient of both types of cell reaches a plateau of about  $10^5$  cm<sup>-1</sup> above 2 eV and drops by a factor  $\sim 10$  between 1.8-2 eV. Direct absorption in the polymer and PCBM therefore occurs above about 1.8 eV. The feature near 1.7-1.8 eV is due to absorption by PCBM. The broad band at lower energy

is the absorption from the polymer HOMO to the PCBM LUMO, across the interface band gap, as illustrated schematically in Fig. 6.

The interface band gap occurs at an absorption coefficient of about  $10 \text{ cm}^{-1}$ , and corresponds to the start of an exponential absorption tail to lower energy [3]. The interface band gap is therefore about 1.2 eV in P3HT:PCBM and about 1.4 eV in PCDTBT:PCBM, which is consistent with the solar cell open circuit voltage, which is typically 0.5-0.6 V below the interface band gap.

The exponentially decreasing absorption tail below the band gap energy has a slope of 37 meV and 45 meV for the two cells respectively. These are the same values as the exponential band tail slope deduced from the transport measurements, within experimental uncertainty, which is a strong indication that they indeed arise from the band tail density of states. The absorption tails are attributed to optical transitions from the band tail of the polymer HOMO to the PCBM LUMO. Transport measurements show that the polymer has a wider band tail than the PCBM, and the optical transitions are dominated by the wider band tail.

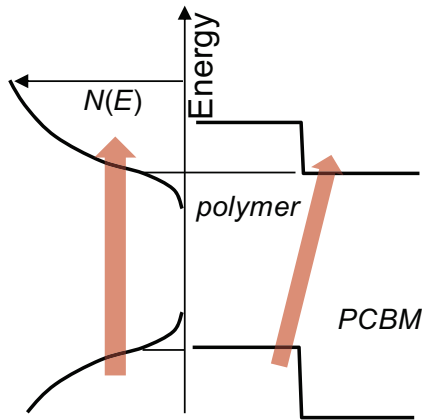


**Figure 6. Schematic illustration of the low energy optical absorption in BHJ solar cells, showing the band alignment of the polymer and PCBM and the bulk and interface absorption transitions.**

#### Absorption due to transitions from deep traps

Figure 7 shows the low energy region of the photoconductivity spectrum in more detail and with higher sensitivity, for a PCDTBT:PCBM cell. The change of slope near 1.1 eV is more visible than in the data of Figure 5 and extends from 1.1 eV down to about 0.8 eV. This region corresponds to optical transitions from the broader distribution of deep states shown in Figure 4. Since the optical absorption is a transition from the trap to a higher energy state, it is a convolution of the deep state distribution with the band edge DOS and hence has a different energy dependence from that of the DOS, as discussed below. The open circles in Figure 7 are the result of a calculation using the model density of states as

discussed below and shows that the optical absorption in low energy region is consistent with the flat DOS of Fig. 4.

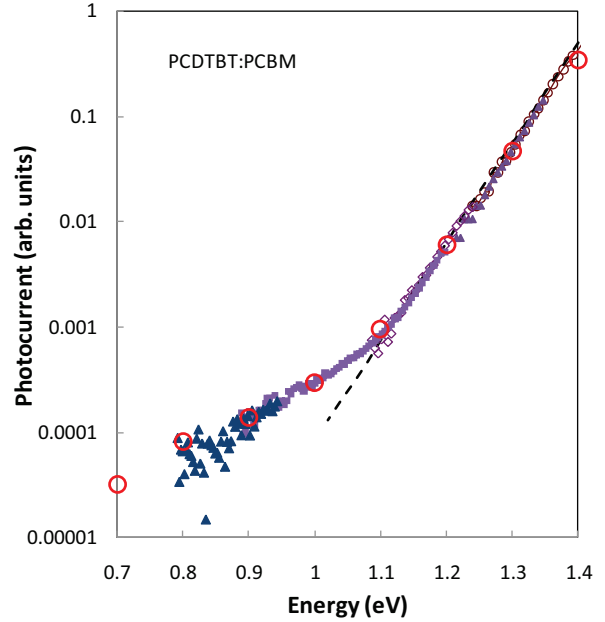


**Figure 7. Spectral response of PCDTBT:PCBM at low photon energy, showing the transitions from deep gap states indicated by the change of slope at 1.1 eV. Open circles are a fit to the model density of states in Figure 8.**

## DISCUSSION AND ANALYSIS

Both the transport and the spectral response experiments give detailed information about the electronic structure, particularly of the localized state distribution and where the measurements overlap they are in good agreement. The transport data provides the exponential band tail slope from the dispersion parameter, and the more detailed density of states distribution from the long time response. The photoconductivity spectral response shows the direct excitations of bulk excitons in the polymer and in the PCBM at high energy, the charge transfer excitations between extended states across the interface band gap, and the transitions across the interface gap associated with the band tails and the deep defects.

#### The density of states distribution

Considerable information about the electronic structure is obtained from the spectral response data of Figures 5 and 7. For example, the magnitude of the band offset, which is the energy difference between the bulk exciton absorption and the interface gap is obtained. The data in Figure 5 indicate a value of about 0.7 eV for the P3HT:PCBM cell and 0.4 eV for the PCDTBT:PCBM cell. The band offset is an important factor limiting the solar

cell's efficiency, and needs to be as small as possible for a high efficiency cell.

Both the transport and the spectral response measurements give the same value for the exponential band tail slope, within experimental uncertainty, and both provide data about the deep trap states. Further modeling studies are needed, but the initial indications are that the two techniques give consistent measurements of the deep trap density and energy distribution.

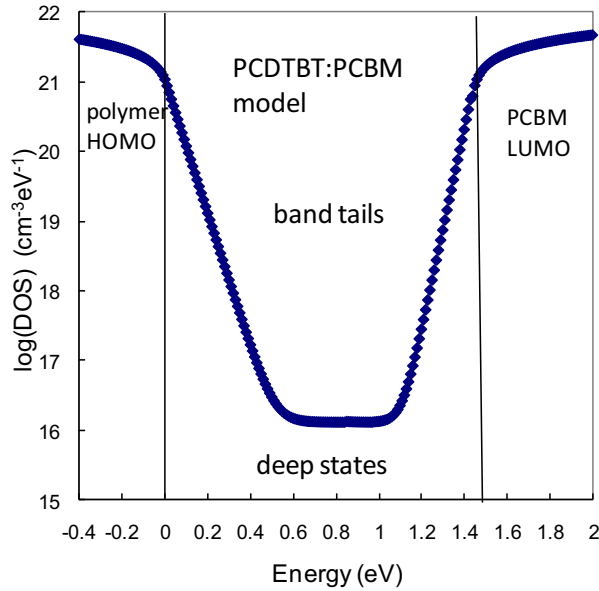


**Figure 8. Model for the density of states  $N(E)$  in PCDTBT:PCBM as a function of energy based on the experimental measurements.**

Figure 8 illustrates a complete model for the density of states distribution in PCDTBT:PCBM, as a function of energy, developed from the measurements described here, together with additional calculations of the density of states within the energy bands of the materials [2]. A similar model for the P3HT:PCBM cell is given in Reference 2. The model shows the HOMO levels of the polymer and the LUMO levels of PCBM. Vertical lines represent the approximate location of the band edges separating mobile transport states from localized states. The interface band gap for PCDTBT:PCBM is approximately 1.4 eV in the model, consistent with the value of the interface band gap is obtained from the spectral response data. The exponential band tails are indicated with a HOMO band tail slope of 45 meV from the experimental data and the LUMO band tail of 30 meV from other data as it cannot be directly measured by the techniques used here. We use a flat density of deep state to approximate the results of Figure 4.

The model is compared to the data by calculating the joint density of states,

$$\alpha_T(\hbar\omega) = cV_F \int \frac{N_V(E)N_C(E+\hbar\omega)|M|^2}{\hbar\omega} dE \quad (4)$$

where  $M$  is the matrix element assumed constant  $V_F$  is the volume fraction of the interface in the bulk heterojunction cell, and  $c$  is a constant.

The calculated joint density of states is shown by the red circles in Figure 7, and its energy dependence accounts well for the change of slope in the spectral response data, providing support for the density of states distribution that was deduced from the transient photoconductivity. The density of deep states used to fit the optical data is smaller than the measured density obtained from the transport data, and perhaps reflects a different matrix element for band-to-band and defect optical transitions.

### Role of DOS in device modeling

The density of states (DOS) is an essential link between the structure and electronic properties of the BHJ cell. The film structure determines the DOS, and in turn, the DOS determines the various electronic properties. The fabrication process to make the cell, the material composition of the device, the phase separation of the components into separate domains and the effects of annealing are all variables. Each of these aspects influences the physical structure and therefore also modifies the electronic structure. A complete knowledge of the device involves understanding how the DOS reflects the atomic and mesoscopic structure of the device, how the DOS influences electronic transport, and what recombination mechanisms are active.

The ability to obtain an experimental measurement of the density of states separates the problem into two parts. The question of how transport and recombination follows from the DOS can be modeled from the DOS without needing a complete knowledge of the actual physical structure. The question of how the electronic properties result from the physical structure can in principle be addressed directly from the measured DOS. It is therefore important and of practical use to obtain the DOS empirically from electronic and optical measurements, as is described here.

### Lifetime and exposure effects

These experimental techniques are the first to provide such specific information about the detailed electronic structure of the bulk heterojunction solar cells. Particular uses of the measured DOS distribution are to allow a comparison between different materials and also to study the change in the DOS with sample preparation and the long term stability. Preliminary measurements indicate that exposure to the ambient introduces additional trap states near the HOMO levels in P3HT:PCBM.

## Recombination mechanisms

In a previous publication we proposed that the dominant recombination mechanism in both these solar cells was through localized states at or near the domain interface [7]. As more evidence for the density of states distribution is obtained, including both the band tails and deep trap states, the significance of transitions through deep states for both the transport and the recombination becomes more apparent. It will be important to quantify the DOS better and to understand the role of the localized states in more detail through device modeling in order to develop new materials that improve the cell efficiency.

## SUMMARY

We have developed experimental techniques to measure the electronic density of states in organic bulk heterojunction solar cells. The results show exponential band tails and deeper localized states. The measurements provide key information to understand electronic transport and to model the transport and recombination. These two experiments allow the changes in the density of states and the corresponding changes in transport and recombination to be measured as a function of cell processing and exposure. Measurement of the density of states will enable a more detailed analysis of the effects of annealing and environmental stability in organic solar cells.

## ACKNOWLEDGEMENTS

The authors are grateful to A. Heeger and S. Cowan for providing the solar cell samples and for useful discussion, to J. Northrup for useful discussion, and to C. Paulson for technical assistance.

## REFERENCES

- [1] S. Gunes, H. Neugebauer and N. S. Sariciftci, "Conjugated polymer-based organic solar cells", *Chem. Rev.* **107**, 2007, p1324.
- [2] R. A. Street, K. W. Song, J. E. Northrup and S. Cowan "Photoconductivity measurements of the electronic structure of organic solar cells", *Phys Rev.*, **B83**, 2011. p165207.
- [2] R. A. Street, "The localized state distribution and its effect on recombination in organic solar cells", submitted to *Phys. Rev.*
- [4] M. Punke, S. Valouch, S. W. Kettlitz, N. Christ, C. Gartner, M. Gerken and U. Lemmer, "Dynamic characterization of organic bulk heterojunction photodetectors" *Appl. Phys. Lett.* **91**, 2007, p071118
- [5] T. Tiedje and A. Rose, "A physical interpretation of dispersive transport in disordered semiconductors" *Solid State Commun.* **37**, 1981, p49-52.

[6] J. Lee, K. Vandewal, S. R. Yost, M. E. Bahlke, L. Goris, M. A. Baldo, J. V. Manca and T. Van Voorhis, "Charge transfer state versus hot exciton dissociation in polymer-fullerene blended solar cells", *J. Am. Chem. Soc.*, **132**, 2010, p11878.

[7] R. A. Street, M. Schoendorf, A. Roy and J. H. Lee, "Interface state recombination in organic solar cells" *Phys. Rev.* **B81**, 2010, p205307.